Journal of Enzyme Inhibition and Medicinal Chemistry, February 2005; 20(1): 25–33

Structural requirements for inhibitors of cytochromes P450 2B: Assessment of the enzyme interaction with diamondoids*

PETR HODEK[1], LUCIE BOŘEK-DOHALSKÁ[1], BRUNO SOPKO[1], MIROSLAV ŠULC[1], STANISLAV SMRČEK[2], JIŘÍ HUDEČEK[1], JOSEF JANKŮ[3], & MARIE STIBOROVÁ[1]

[1]*Department of Biochemistry, Faculty of Science, Charles University, Hlavova 2030, Prague 2 CZ-12840, Czech Republic,* [2]*Department of Organic Chemistry, Faculty of Science, Charles University, Hlavova 2030, Prague 2 CZ-12840, Czech Republic, and* [3]*Department of Environmental Chemistry, Prague Institute of Chemical Technology, Technická 5, Prague 6 CZ-16628, Czech Republic*

(Received 4 May 2004; in final form 14 October 2004)

Abstract

The series of diamondoids: adamantane, diamantane, triamantane, 2-isopropenyl-2-methyladamantane and 3-isopropenyl-3-methyldiamantane (3-IPMDIA), were employed to elucidate the molecular basis of their interaction with the active site of cytochromes P450 (CYP) of a 2B subfamily. These potent inhibitors of CYP2B enzymes were docked into the homology model of CYP2B4. Apparent dissociation constants calculated for the complexes of CYP2B4 with docked diamandoids agreed closely with the experimental data showing inhibition potency of the compounds and their binding affinity to CYP2B4. Superimposed structures of docked diamondoids mapped binding site residues. As they are mainly non-polar residues, the hydrophobicity plays the major role in the binding of diamondoids. Overlapping structure of diamondoids defined an elliptical binding cavity (5.9 Å inner diameter, 7.9 Å length) forming an angle of ~43° with the heme plane. CYP2B specific diamondoids, namely 3-IPMDIA, showing the highest binding affinity, should be considered for a potential clinical use.

Keywords: *Cytochrome P450 2B, CYP2B4, enzyme inhibition, diamondoid compound, homology model, substrate binding*

Abbreviations: *ADA, adamantane; CHAPS, 3-[(3-cholamidopropyl)dimethyl-ammonio]-1-propane sulfonate; CYP, cytochrome P450; DIA, diamantane; DMSO, dimethyl sulfoxide; IC_{50}, inhibitor concentration causing 50% of inhibition; Ki, inhibition constant; Km, Michaelis constant; Ks, spectral dissociation constant; Kd, kinetic dissociation constant; K/PO_4, potassium phosphate; PB, Phenobarbital; PROD, 7-pentoxyresorufin O-depentylation; TRIA, triamantane; 2-IPMADA, 2-isopropenyl-2-methyladamantane; 3-IPMDIA, 3-isopropenyl-3-methyldiamantane*

Introduction

The cytochrome P450 (CYP) monooxygenases are heme-containing mixed-function oxidases playing a key role in metabolism of mostly hydrophobic endogenous substrates (sterols, prostaglandins, fatty acids) and ingested foreign compounds, xenobiotics, (e.g. drugs, carcinogens, food components, pollutants) [1]. Although CYPs generally convert xenobiotics to less toxic products, the reactions frequently involve the formation of reactive intermediates or the leakage of free radicals capable of causing toxicity or carcinogenicity [2]. Thus, the inhibition of CYPs seems to be logical to prevent the CYP-mediated carcinogen activation and/or chemical toxification. Naturally occurring compounds, flavonoids, for example, have been recognized as chemopreventive agents acting as effective inhibitors of several CYPs metabolizing xenobiotics, namely: CYP1A1, 1A2, 1B1 and 3A4, and one steroidogenic CYP19 [3]. Moreover, some drugs, i.e. ketoconazole and troleandomycin, are efficient inhibitors of CYP3A4, the most abundant

Correspondence: P. Hodek, Department of Biochemistry, Faculty of Science, Charles University, Hlavova 2030, Prague 2 CZ-12840, Czech Republic. Tel: 420 2 21951285. Fax: 420 2 21951283. E-mail: hodek@natur.cuni.cz

*Dedicated to Professor Sylva Leblová

ISSN 1475-6366 print/ISSN 1475-6374 online © 2005 Taylor & Francis Ltd
DOI: 10.1080/14756360400024324

human CYP [4]. Though, CYP2B6, another member of the human multigene family, is generally regarded as a minor CYP [5], it catalyzes the oxidation of various xenobiotics including drugs and carcinogens such as nicotine [6], aflatoxin B1 [7], styrene [8] and aminochrysene [9]. However, selective and potent inhibitors of CYP2B6 have not yet been established. There have been few reports describing the inhibitors of CYP2B6 (e.g. diethyldithiocarbamate, 4-methylpyrazole, quercetin, ellipticine, troleandomycin, methoxsalen) [10], however, the results suggest that none of these are selective inhibitors of this enzyme at the concentrations used [11]. Only recently, compounds of diamond-like structure (diamondoids), recognized as highly specific substrates of rat CYP2B1 and rabbit CYP2B4 [12–16], were proved to inhibit human CYP2B6-mediated formation of tamoxifen-DNA adducts, which are responsible for carcinogenic tamoxifen side-effects [17]. Hence, these compounds warrant consideration as candidates for preventing endometrial cancer development in humans treated with this drug.

Due to the general importance of CYPs in carcinogen bioactivation and drug metabolism, elucidation of the key structural elements responsible for inhibitor and substrate recognition and consequent binding to the CYP active center is of considerable interest [18]. Understanding the principle of CYP binding specificity is essential because of their clinically important role in the metabolism of xenobiotics and endogenous compounds. However, our knowledge of this process has been limited by the lack of three-dimensional (3D) structures for mammalian CYPs. Until recently, the membrane-bound microsomal CYPs have not been amenable to crystallography, making it necessary to utilize other approaches to obtain structure-function data on mammalian enzymes. Since tertiary structure appears to be conserved throughout the CYP superfamily [19], hypothetical 3D molecular models of mammalian CYPs have been constructed based on analogy to the known crystal structures of bacterial CYPs [20]. Homology modeling has become an essential tool in understanding the structural basis of CYP function [21]. Although crystal structures of the truncated, solubilized rabbit CYP2C5, 2C9 and 2B4 are now available [22–24], structural data provided by other approaches are still important. That is why it is hard to rule out the possibility that in the CYP crystal some perturbations of CYP native structure might occur as a consequence of significant structural changes prior to the microsomal CYP crystallization (elimination of N-terminal transmembrane domain, modification of N-terminus, addition of C-terminal 4xHis tag) and/or caused by the process of crystallization itself (e.g. CYP dimerization). The reported crystal structure of rabbit CYP2B4 shows an unusually large open cleft (extended to the heme moiety) that is trapped by homodimer formation [24]. This open conformation does not agree with photoaffinity labeling data, obtained with the native enzyme in solution, and some data from the site-directed mutagenesis [25–28]. It is not known whether the wild type of CYP2B4 is also able to adopt the open conformation, seen in the crystal of truncated substrate-free CYP2B4 [24].

Thus, homology modeling is a well applicable alternative for structural studies of CYP2B enzymes [29–32]. This technique in conjunction with data from other structural studies (e.g. site-directed mutagenesis) allows insight into the relationship between CYP structure and function, providing a base for rational inhibitor and drug design. It may also help to predict the possible metabolic fate of drugs and carcinogens in organisms.

In this study, the interactions of potential inhibitors of CYP2B enzymes, adamantane (ADA), diamantane (DIA), triamantane (TRIA) and two derivatives, 2-isopropenyl-2-methyladamantane (2-IPMADA) and 3-isopropenyl-3-methyldiamantane (3-IPMDIA) (Figure 1) with these enzymes was examined. Using the new generation homology model of CYP2B4 verified experimentally, binding of these compounds to the enzyme active center was explored on a molecular basis. Results of "*in silico*" docking of diamondoid compounds, as well as kinetic, inhibition and binding assays revealed that 3-IPMDIA is the most efficient inhibitor of CYP2B among compounds tested in this study. Structural determinants of CYP2B, governing diamondoid binding and inhibition, are discussed.

Materials and methods

Chemicals

7-Pentoxyresorufin and 7-hydroxy-4-trifluoromethylcoumarin were purchased from Fluka Chemie AG (Switzerland). 7-Ethoxy-4-trifluoromethylcoumarin, glucose 6-phosphate, $NADP^+$, NADPH, 3-[(3-cholamidopropyl)dimethylammonio]-1-propane sulfonate (CHAPS), dilauroyl phosphatidylcholine and dithiothreitol were obtained from Sigma Chemical Co. (St. Louis, MO, USA). Dimethyl sulfoxide (DMSO) and methanol were purchased from Merck (Darmstadt, Germany). Phenobarbital was from Kulich Co. (Hradec Králové, Czech Republic). Glucose 6-phosphate dehydrogenase was from Serva (Heidelberg, Germany). Bicinchoninic acid was from Pierce (Rockford, IL, USA). All chemicals were of a reagent grade or better. Adamantane, diamantane and triamantane were obtained from J. Janků and J. Burkhard (Prague Institute of Chemical Technology, Praha, Czech Republic). 2-IPMADA and 3-IPMDIA were synthesized according to Olah *et al.* [33] (purity 99.8%). Supersomes™, microsomal samples isolated from insect cells transfected with baculovirus co-expressing human CYP2B6 enzyme and

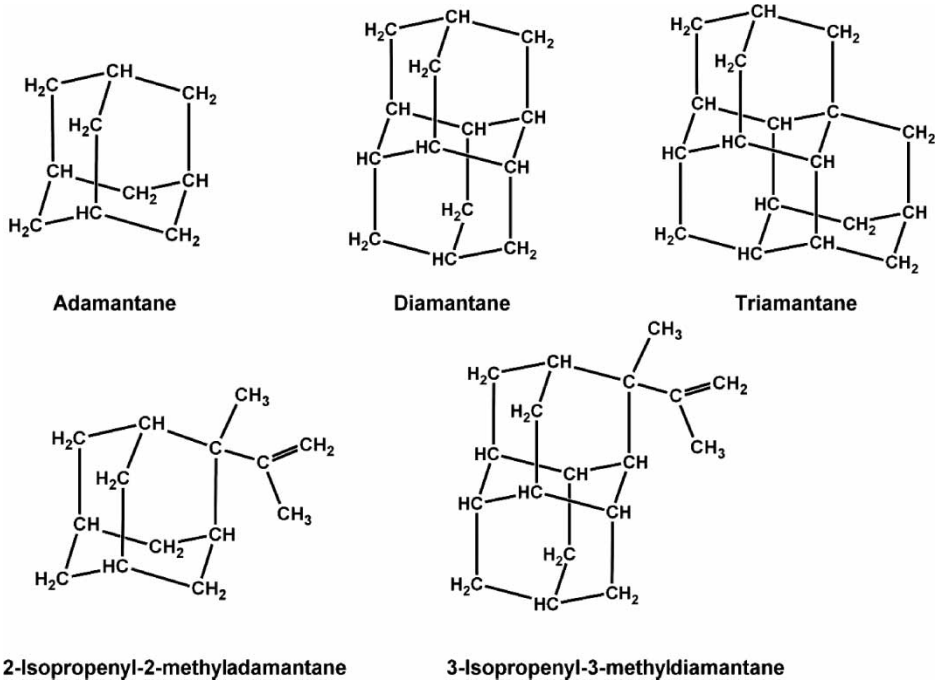

Figure 1. Structure of diamond-like compounds.

NADPH:CYP reductase, were from Gentest Corp. (Woburn, MA).

Animal pretreatment

Adult male rabbits (2.5–3.0 kg) and male Wistar rats (150–200 g) were fed *ad libitum* on pellet chow and water one week before treatment. Rabbits and rats were pretreated with phenobarbital (0.1% in drinking water for 6 days) to induce liver CYP2B enzymes. Animals were killed after 18 h of starvation by cervical dislocation.

Preparation of microsomes and isolation of CYP enzymes

Microsomes were isolated from the livers of rabbits and rats pretreated with phenobarbital by procedures described previously [34] and stored at − 80°C. Total CYP content was measured based on the complex of reduced CYP with CO [5]. CYP2B4 and CYP2B2 were isolated from the liver microsomes of rabbit and rat induced by phenobarbital as described earlier [25, 36]. Rabbit liver NADPH:CYP reductase was purified as described by Hodgson and Strobel [37]. The activity of NADPH:CYP reductase was measured according to Williams and Kamin [38] using cytochrome c as a substrate. The concentration of NADPH:CYP reductase was estimated as described earlier [39]. Protein concentration was determined using the bicinchoninic acid protein assay with bovine serum albumin as a standard [40].

Enzyme assays

CYP2B specific activity, 7-pentoxyresorufin O-dependentylation, was measured in 1 ml reaction mixture containing: 0.1 M K/PO_4, pH 7.4, 0.25–5 μM 7-pentoxyresorufin, 0.25 mM NADPH and 0.1 μM CYP present in microsomes isolated from the liver of rats and rabbits pretreated with PB (PB-microsomes). After 10 min incubation at 37°C (shaking incubator) the reaction was terminated by 2 ml of methanol. The amount of resorufine formed was measured fluorometrically using a Perkin Elmer LS-5B spectrofluorometer [41]. Reconstitution of CYP2B2 and CYP2B4 with NADPH:CYP reductase was carried out using 0.5 μM CYP2B, 0.5 μM NADPH:CYP reductase, 0.5 mg/ml CHAPS, 0.1 mg/ml liposomes (D,L-dilauroylphosphatidylcholine), 3 mM reduced glutathione and 50 mM HEPES/KOH, pH 7.4 followed by 7-pentoxyresorufin O-dependentylation assay [42]. The activity of CYP2B6 was determined fluorimetrically in a reaction mixture containing 0.04 μM CYP (present in Supersomes™), 0.1 mM 7-ethoxy-4-trifluoromethylcoumarin and a NADPH-generating system in 0.1 M K/PO_4, pH 7.4, as described earlier [17].

Inhibition studies

The inhibitory effect of diamondoid compounds, ADA, DIA, TRIA, 2-IPMADA and 3-IPMDIA on individual CYP2B enzymes (present in microsomes isolated from the livers of rats or rabbits pretreated with PB, Supersomes™ or reconstituted CYP enzymes of a 2B subfamily) 7-pentoxyresorufin O-dependentylation or 7-ethoxy-4-trifluoromethylcoumarin deethylation was determined in the presence of 0.17–150 μM concentrations of these compounds and NADPH.

All diamondoid compounds were applied to the reaction mixture as DMSO stock solutions. The IC_{50} values were estimated from concentration curves by interpolation and Ki values from Dixon plots as described earlier [43].

Spectral binding studies

Interaction of cytochrome P450 with diamondoid compounds was followed by difference spectroscopy (Specord M-40, M-42, Carl Zeiss, Jena, Germany) [44]. PB-induced microsomes and pure CYP2B enzymes were diluted with 0.1 M K/PO_4 buffer, pH 7.4 to 3.3 μM and 2 μM CYP, respectively. After recording the "base-line", the CYP in the sample cuvette was perturbated with gradually increasing amounts of diamondoid compound (0.1–50 μM). The same volume of the compound solvent (methanol), not exceeding 2% of total volume, was added to the reference cuvette. The resulting high–low spin shift of heme iron was monitored as difference spectra from 350 to 500 nm [45]. Spectral dissociation constants (Ks) were determined as described elsewhere using a nonlinear regression method (Origin 6.0 software) [17].

Docking experiments

The three-dimensional structure of rabbit CYP2B4 was built based on the crystal structures of CYP2C5 [22], CYP51 [46], and CYP102 [47] as described previously [32]. Briefly, after the generation of sequence alignment (Modeller 6.2, ClustalX) the known structures were spatially aligned (Modeller 6.2) and the loop residues were added to the CYP2C5 sequence. Finally, the CYP2B4 was aligned from N-terminal residue 45 to the created alignment among CYP51, CYP102, and CYP2C5 and the F-G loop in CYP2B4 was constructed. After the heme group docking the structure had been subjected to several energy minimizations.

All of the substrate structures were docked into the model. For docking the Autodock 3.05 software was employed, using the genetic algorithm method, with 27000000 generations and 200 populations, with 20 runs for each substrate [48]. The conformation having the lowest energy was chosen as the result.

Results and discussion

Cytochromes P450 (CYP) of a 2B subfamily show strong preferences for binding of "bulky" compounds having a low value of compound area/depth^2 ratio and rather high compound volume [49]. That is why, highly hydrophobic compounds of diamond-like structures, adamantane (ADA) and diamantane (DIA), are well accommodated by rat CYP2B1 and rabbit CYP2B4 [12,36]. In order to understand further the structural determinants driving CYP2B substrate binding and investigate the shape and size of the CYP2B binding site, additional compounds were employed in the present study. Namely, another member of the diamondoid series, triamantane (TRIA), a molecule containing one diamond crystal cage more than DIA, and derivatives of two former compounds, 2-isopropenyl-2-methyladamantane (2-IPMADA), and 3-isopropenyl-3-methyldiamantane (3-IPMDIA) [17], were utilized in the study. Structures of diamondoid compounds used are depicted in Figure 1. Results of their docking into the enzyme active site of a CYP2B4 model structure in combination with data from metabolic (inhibition) and binding assay (spectral substrate titration) studies, focused on CYP2B4, provided an insight into CYP binding site topology of this enzyme and allowed us to explain features of its interactions with substrate/inhibitor.

Spectral binding studies of diamondoid compounds

Using difference spectroscopy, the interaction of CYPs with compounds of the diamondoid structure was monitored. These experiments were carried out using liver microsomes of rats and rabbit enriched in CYP2B1/2 and 2B4, respectively, after animal treatment with phenobarbital (strong inducer of CYP2B enzymes). All the compounds elicited substrate binding spectra of type I with typical absorption extremes: maximum at about 390 nm and minimum at 421 nm [12,44]. An analysis of the difference spectra revealed an apparent spectral dissociation constant (Ks), reflecting the enzyme binding affinity for the respective compound. The values of this spectral binding parameter are shown in Table I. When Ks values for the series of non-substituted diamondoid compounds ADA, DIA, TRIA are compared, it is obvious that diamantane appears to be the compound with the highest affinity for CYP2B4 binding in the microsomal samples. To gain more detailed information on structural requirements of the enzyme binding site, derivatives of ADA and DIA having an increased

Table I. Spectral dissociation and inhibition constants of diamondoid compounds.

Compound	Rabbit PB-microsomes		Purified CYP2B4
	Ks [μM]	Ki [μM]	Ks [μM]
ADA	9.75	4.36	1.57
2-IPMADA	2.24	1.95	0.59
DIA	0.83	0.81	0.50
3-IPMDIA	0.44	0.33	0.19
TRIA	0.89	1.61	0.40

Ks, spectral dissociation constant; Ki, inhibition constant. Numbers in the Table are the average of three parallel experiments (standard deviations were less than 10%).

molecular size, 2-IPMADA and 3-IPMDIA, were used in further experiments. The data listed in Table I demonstrate the increased binding affinities of CYP2B4 for both isopropenylmethyl-derivatives in comparison to the parent adamantane and diamantane. The same conclusion could be drawn from results obtained with the liver microsomes of PB-treated rats (data not shown). To exclude the involvement and/or interference of other CYPs (present in microsomes) on the diamondoid binding experiments with purified CYP2B4 were carried out. Ks values determined with the pure enzyme (Table I) confirmed, in accordance with the preceding results, a pronounced preference of the CYP2B4 binding site for 3-IPMDIA. Differences between both sets of Ks values for microsomes and purified CYP2B4 are likely to be associated with the substrate hydrophobicity that appears to be a common feature, especially, for microsomal CYPs. It is thought that membrane interactions play an important role in the process of substrate binding [49]. As shown in our previous study, also in systems containing purified rat CYP2B2 or human CYP2B6 in Supersomes™, 3-IPMDIA was proven to be the compound with the lowest Ks of all the diamondoids tested.

Inhibition of CYP2B enzymes by diamondoid compounds

To confirm the observation that 3-IPMDIA best fits to the enzyme binding cavity of CYP2B enzymes, its ability to inhibit oxidation of CYP2B substrates, 7-pentoxyresorufin for CYP2B1/2/4 and 7-ethoxy-4-trifluoromethylcoumarin for CYP2B6, was determined. Table I summarizes values of the inhibition constants (Ki) determined for the whole set of diamondoid compounds with the rabbit experimental system. The presence of the isopropenylmethyl-moiety in the diamondoids, ADA and DIA, led to their improved inhibition efficiency. Thus, in accordance with data from binding experiments, the most effective inhibitor of CYP2B4 enzymatic activity is 3-IPMDIA. Further increase in the molecular size of a diamondoid structure results in impaired binding to the enzyme active center and, consequently, in an enhanced Ki, determined in the case of triamantane. To further clarify that 3-IPMDIA binds strongest to CYP2B, the inhibition experiments were performed also with purified CYP2B4 reconstituted with NADPH:CYP reductase. The determined Ki values of 2.09 and 0.27 μM for 2-IPMADA and 3-IPMDIA, respectively, were very similar to those determined in the microsomal system. The Ki values of 5.27 and 2.17 μM for 2-IPMADA and 3-IPMDIA, respectively, were found for CYP2B6. Although they are one order of magnitude higher than for CYP2B4, they are still micromolar and indicate strong affinity for CYP2B6 [17].

Both isopropenylmethyl-compounds (2-IPMADA and 3-IPMDIA) were shown to be metabolized into mono-, di- and trihydroxy-derivatives, like non-substituted diamondoids, when incubated with rabbit PB-microsomes [17]. These experiments revealed Km values of 128 and 92 μM, for 2-IPMADA and 3-IPMDIA, respectively [17]. The Km values for both compounds are several order of magnitude higher than their Ks values, as well as relatively slow rates ($\sim 1\,min^{-1}$) for their oxidation suggesting these diamondoids to be poorly metabolized by enzymes of a CYP2B subfamily.

Diamondoid docking in CYP2B4

In order to explain the molecular basis of interactions of diamondoid compounds with the active center of CYP2B enzymes information on their 3D structure are necessary. However, the recent crystal structure of rabbit CYP2B4 [24] (revealing an unusual open conformation) places several predicted active-site key residues in locations less compatible with substrate binding/turnover. Moreover, the location of the C-helix in the open conformation alters the site proposed to be important for binding of NADPH-CYP reductase and cytochrome b_5. That is why, the new homology model of CYP2B4 [32], based mainly on the crystal structure of CYP2C5, was utilized to elucidate structural features of diamondoid compounds determining CYP2B inhibition. The confidence that the homology model corresponds to the native structure of a CYP2B4 active center has been gained by projecting the experimental data of photoaffinity labeling and diamantane metabolism to the CYP2B4 theoretical structure [25,32]. Thus, the evaluated CYP2B4 model was chosen to serve as a 3D prototype structure of the highly homologous CYP2B enzyme subfamily. This type of structural data is important for the orthologous human CYP2B enzyme, CYP2B6, because there is still no crystal structure for this membrane-bound human CYP.

Docking of the test set diamondoids revealed amino acid residues lining the active site of the CYP2B4 model within a distance of 4 Å from the diamondoid carbon skeletons (see Table II). From the twelve identified residues only two, Asp105 and Thr302, are polar. Most of these residues identified in this study match those which have been predicted previously by mutagenesis and modeling studies to be important for substrate binding or catalytic activities of the CYP2B subfamily [27,30,50]. Mapped residues (Ile114, Ile363), making close contact with the isopropenylmethyl moiety of 3-IPMDIA, have also been found to be critical for CYP2B4 inhibition [28]. The involvement of two hydrophobic residues, Leu199 and Leu201, in substrate/inhibitor binding have not previously been suggested. In our 3D model structure these residues are located in the upper part of the binding site cavity, close to the access channel opening. The closest predicted active site amino acid

Table II. Key active site amino acid residues of CYP2B4 model structure in contact with diamondoids.

Sequence position		CYP2B4 amino acid residue				
		ADA	2-IPMADA	DIA	3-IPMDIA	TRIA
101	[30]	–	Ile**	Ile**	**Ile****	Ile**
105	[30]	–	Asp	Asp	Asp	Asp*
114	[27,31]	Ile**	**Ile***	Ile*	Ile**	Ile*
115	[27]	–	Phe	Phe	Phe	Phe
199	–	–	–	–	**Leu***	Leu*
201	–	–	–	–	**Leu***	Leu*
297	[30]	Phe*	Phe*	Phe*	**Phe***	Phe*
298	[27]	Ala*	**Ala***	Ala	Ala*	Ala**
302	[27]	Thr*	**Thr****	**Thr***	Thr*	Thr*
363	[27,31]	Ile*	Ile*	Ile*	**Ile***	Ile*
367	[27]	–	Val*	Val*	Val	Val**
477	[27]	Val*	**Val***	Val**	Val**	Val**

Listed amino acid residues are within 4 Å distance (residues marked by asterisks * and ** are within 3.5 and 3.0 Å, respectively) from the diamondoid carbon skeleton. Residues interacting with the isopropenylmethyl-moiety are in bold letters. References to papers predicting that the amino acid residue is at the active center are shown in parenthesis.

residues, Phe202 and Phe206, spanning to helix F, were suggested by Chang *et al.*, [29,50] (based on the homology modeling approach). It is interesting to note that although diamondoids of increasing size were docked in the active site, the side chains of the active site amino acid residues did not have to move to accommodate them. As judged by the values of the apparent dissociation constants (Kd) calculated for the complexes of CYP2B4 with docked diamondoid compounds (Table III) all these diamondoids (with the exception of ADA) made a good fit with the substrate binding cavity of the CYP2B4 model. The Kd values agreed well with experimentally determined Ks and Ki values for with native CYP2B4 in microsomes. Correlation coefficients (Table IV) of 0.993 for Kd and Ks values, and 0.931 for Kd and Ki show a close relation of both sets of experimental data with Kd values. On the other hand, when the CYP2B4 crystal [24] is used for the docking, the calculated values of Kd (see Table III) differ significantly from those of Ks (or Ki) determined experimentally. Correlation coefficients of the CYP2B4 crystal structure shown in Table IV clearly document a looser correlation of theoretical and experimental data in comparison with the homology model of the CYP2B4 protein molecule.

Assessment of docked diamondoids

Although there is considerable structural diversity in CYP substrates, hydrophobicity appears to be a common feature, especially for microsomal CYPs, where it is thought that membrane interactions play an important role [49]. All diamond-like compounds tested in the present study are of highly hydrophobic structures. The first compound of the diamondoid series, ADA, having the highest Ks, Ki and Kd values, seems to be loosely bound in the active center of CYP2B4. ADA docked in the active center is oriented in accordance with metabolic data since it is facing the apical carbon atom (C1) which undergoes hydroxylation to the heme [51]. The ADA skeleton is in contact (distance 3–4 Å) with only six of the twelve side chains of the active site amino acid residues. Desolvation energies tend to equate with substrate hydrophobicity which are, to the some extent, related to the size of the relevant CYP active site and, also, to that of the substrate itself [49]. Thus, ADA of

Table III. Binding parameters of diamondoid compounds docked in CYP2B4 structures.

Compound	Volume [Å^3]	CYP2B4 model		CYP2B4 crystal	
		Estimated Kd [μM]	Docked E [kcal/mol]	Estimated Kd [μM]	Docked E [kcal/mol]
ADA	145	41.3	−5.98	28.1	−6.21
2-IPMADA	207	3.9	−7.71	20.1	−6.74
DIA	196	1.7	−7.88	4.3	−7.33
3-IPMDIA	256	1.2	−8.08	8.1	−7.21
TRIA	238	1.9	−7.82	1.0	−8.17

Kd, apparent dissociation constant calculated from docking; Docked E, free energy of binding.

Table IV. Correlation analysis of diamondoid binding and inhibition parameters with apparent dissociation constants Kd of CYP2B4 model and crystal structures.

	Correlation coefficients			
	CYP2B4 model		CYP2B4 crystal	
Correlated values	Kd vs. Ks	Kd vs. Ki	Kd vs. Ks	Kd vs. Ki
Experimental system:				
PB-microsomes	0.993	0.931	0.853	0.813
Purified CYP2B4	0.972	nd	0.820	nd

Kd, estimated dissociation constant; Ki, inhibition constant; Ks, spectral dissociation constant; nd, not determined. Correlation coefficients were calculated using a built-in module of Microsoft Excel 97.

a relatively low hydrophobicity (and small size) shows a poor fit with the substrate binding cavity. That is why it is probably less effective in water molecules displacement and consequently in the heme iron spin shift that is detectable by difference spectroscopy (Ks). Introduction of isopropenylmethyl moiety to the ADA structure resulted in stronger binding to the homology model of the CYP2B4 enzyme. An increased number of contacting hydrophobic amino acid residues to nine is reflected in a significantly lowered Kd value (compared to that of ADA). The isopropenylmethyl group of docked 2-IPMADA is facing heme, while the ADA skeleton is rotated and moved further from the heme. Thus, the size of 2-IPMADA matches better with the enzyme binding site than the parent compound. These theoretical results are consistent with data from spectral titration and inhibition studies showing a 2–4 fold decrease in the Ks and Ki values for 2-IPMADA (relative to ADA). It is worth noticing that in contrary to the present data, the docking of ADA and 2-IPMADA to the crystal structure of CYP2B4 [24] revealed unexpectedly close Kd values 28.1 and 20.1 μM, respectively. Docking of the next member of the diamondoids, DIA, to the CYP2B4 model structure resulted in DIA orientation relative to the heme allowing a preferred apical C4-hydroxylation that has also been determined experimentally [12] The DIA, similarly to 2-IPMADA, is able to map the same active center amino acid residues of CYP2B4. According to Kd, Ks and Ki values the DIA molecule better complies to the size and shape of the enzyme binding site than 2-IPMADA. In addition, the effect of ADA substitution with the isopropenylmethyl moiety that markedly elevated its binding affinity was also tested with the DIA skeleton. Resulting 3-IPMDIA showed elevated binding affinity (based on Kd value) compared to DIA. In contrast to 2-IPMADA, the isopropenylmethyl group is pointing away from the heme towards the substrate access channel. All twelve contact active site residues are within a distance of 4 Å from the 3-IPMDIA skeleton (see Figure 2). The structure of 3-IPMDIA complements the binding site of the CYP2B4 model very well. There is close contact of the isopropenylmethyl group with five hydrophobic active site residues (Ile101, Leu199, Leu201, Phe297, Ile363) that contribute significantly to the strength of the binding interaction. That is why this compound is the most potent inhibitor of CYP2B4-mediated oxidation of substrates as well as the substrate with the highest binding affinity in spectral titrations of all the diamondoids tested. TRIA, having a compact "V"-like structure composed of three diamond crystal cages, seems to be rather bulky to be accommodated in the binding cavity. Thus, the reason for slightly impaired inhibition capacity and binding affinity most likely originates from the TRIA size/shape, which, to some extent, exceeds the structural restrains of the active site, which are achieved by the other diamondoids.

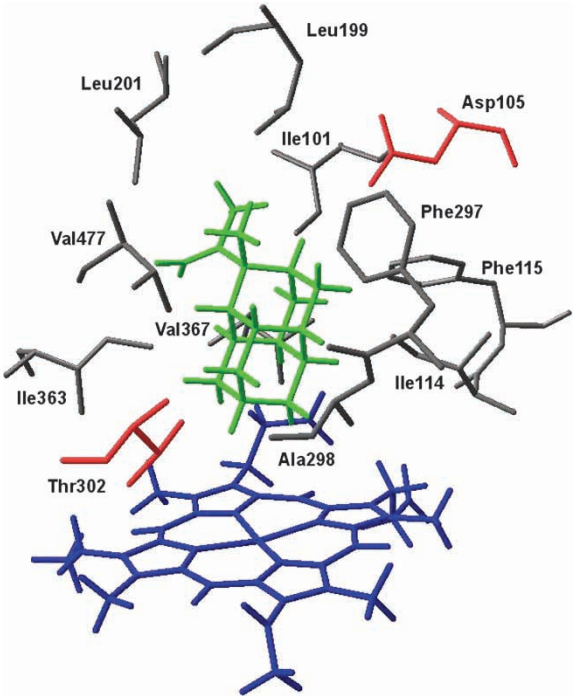

Figure 2. The active site of CYP2B4 model with docked 3-isopropenyl-3-methyldiamantane (3-IPMDIA). Amino acid residues (polar in red) lining the substrate binding cavity within a distance of 4 Å from the carbon skeleton of 3-IPMDIA (in green) are presented.

Inhibitor template structure

Docking of all diamondoids into the CYP2B4 model revealed the topology of the active site and the character of key amino residues, which are the major determinants of the binding. As both the side-chains of residues and diamondoids are non-polar, the contacts formed by the protein and these compounds are predominantly hydrophobic. On the other hand, docking data also predicted plausible orientation of diamondoids in the CYP2B4 active center. When overlapping their docked structures a prototype molecular template of well accommodated compound was generated (see Figure 3). The compound of such a bulky structure and a molecular volume of 320 Å^3 should exert an excellent inhibitory capacity. Focusing on the diamondoid skeletons of diamondoids with the highest binding affinity, the active site space occupied by them might be approximated as an elliptical structure with an internal diameter and length of 5.9 Å and 7.9 Å (including H atoms), respectively. The closest distance of the carbon skeleton from the heme iron is 4.6 Å. A longitudinal axis of the elliptical structure forms an angle of ~43° with the plane of heme. While ADA, DIA, TRIA, 2-IPMADA and the DIA skeleton of 3-IPMDIA span the described elliptical structure, the isopropenyl group of 3-IPMDIA partially exceeds that common structure (see Figure 4). However, the isopropenylmethyl moiety brings about a further increase in the binding affinity by interaction with residues Ile101, Leu199, Leu201, Phe297 and Ile363 in its close vicinity.

In the process of preparation of this paper several articles reporting mammalian CYP crystal structures appeared [54–56]. Readers are advised to review the CYP2B4 "closed structure" obtained in the presence of 4-(4-chlorophenyl)imidazole [56] to get the entire view of the actual knowledge of this CYP structural feature.

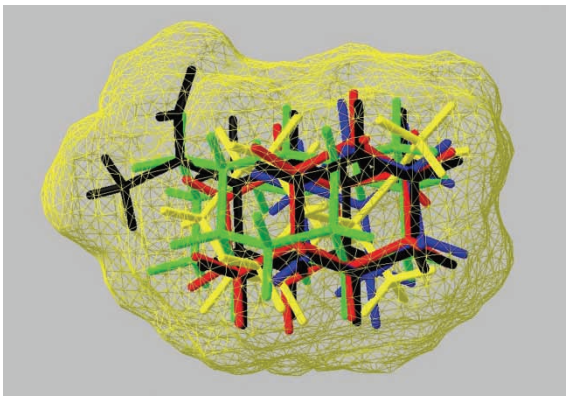

Figure 3. Template structure generated by superposition of docked diamondoids: ADA (blue), 2-IPMADA (yellow), DIA (red), 3-IPMDIA (black), TRIA (green).

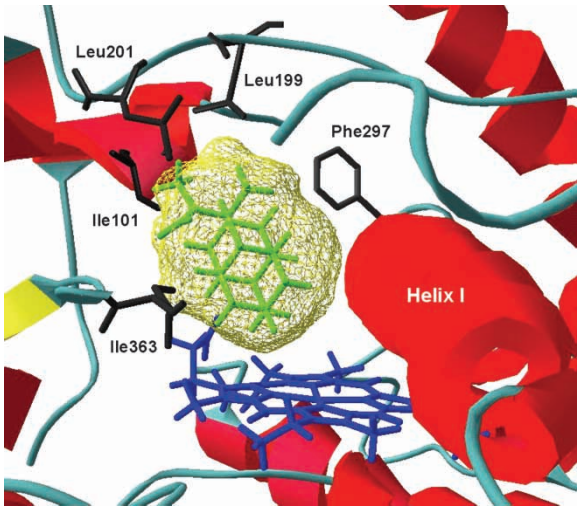

Figure 4. View of the CYP2B4 binding cavity with the heme (in blue) showing the elliptical structure (in yellow) approximating docked diamondoids. The isopropenylmethyl moiety of 3-IPMDIA (in green) makes a close contact with binding site amino acid residues Ile101, Leu199, Leu201, Phe297 and Ile363.

Conclusion

The docking of diamondoid compounds to the CYP2B4 model in combination with metabolic and binding studies provides detailed knowledge of the molecular basis of the interaction of compounds with the enzyme active site. It helps to establish a base for the rational design of selective inhibitors for CYP2B subfamily enzymes. The DIA derivative, 3-IPMDIA, was confirmed to be a potent inhibitor of rabbit CYP2B4, rat CYP2B2 and human CYP2B6 [17]. As a result of the postulated role of CYP2B in the metabolism of several drugs or in activation of some carcinogens [11], selective inhibition of CYP2B may regulate pharmacological or carcinogenic potencies of such compounds. While 3-IPMDIA showed strong inhibition of CYP2B with high selectivity towards these CYP enzymes, this compound seems to be ineffectively metabolized by CYP2B as judged by the relatively slow rate of their oxidation (~1 min^{-1}). This observation is of high significance since potential inhibitors derived from the diamondoid skeleton may persist in an organism long enough to exert their therapeutic effects. Thus, along with diamondoid compounds already used as antiviral agents (e.g. against influenza infection) [52] and in the management of Parkinson's disease [53], 3-IPMDIA, showing a high selectivity and inhibition potency towards CYP2B, might have a future clinical use.

Acknowledgements

The work was supported by Grant MSM-113100001 from The Czech Ministry of Education. We thank Dr Martinek for optimizing diamondoid structures.

References

[1] Nebert DW, Dieter MZ, Pharmacology 2000;61:124–135.
[2] Guengerich FP, Pharmacol Ther 1992;54:17–61.
[3] Hodek P, Trefil P, Stiborová M, Chem Biol Interact 2002;139:1–21.
[4] Halpert JR, Guengerich FP, Bend JR, Correia MA, Toxicol Appl Pharmacol 1994;125:163–175.
[5] Shimada T, Yamazaki H, Mimura M, Inui Y, Guengerich FP, Pharmacol Exp Ther 1994;270:414–423.
[6] Schoedel KA, Tyndale RF, Biochim Biophys Acta 2003;1619:283–290.
[7] Kirby GM, Wolf CR, Neal GE, Judah DJ, Henderson CJ, Srivatanakul P, Wild CP, Carcinogenesis 1993;14:2613–2620.
[8] Nakajima T, Elovaara E, Gonzalez FJ, Gelboin HV, Raunio H, Pelkonen O, Vainio H, Aoyama T, Chem Res Toxicol 1994;7:891–896.
[9] Yamazaki H, Mimura M, Oda Y, Inui Y, Shiraga T, Iwasaki K, Guengerich FP, Shimada T, Carcinogenesis 1993;14:1271–1278.
[10] Ono S, Hatanaka T, Hotta H, Satoh T, Gonzalez FJ, Tsutsui M, Xenobiotica 1996;26:681–693.
[11] Ekins S, Wrighton SA, Drug Metab Rev 1999;31:719–754.
[12] Hodek P, Janščák P, Anzenbacher P, Burkhard J, Janků J, Vodička L, Xenobiotica 1988;18:1109–1118.
[13] Hodek P, Burkhard J, Janků J, Gen Physiol Biophys 1995;14:225–239.
[14] Stiborová M, Schmeiser HH, Wiessler M, Frei E, Cancer Lett 1999;138:61–66.
[15] Hodek P, Smrček S, Gen Physiol Biophys 1999;18:181–198.
[16] Bořek-Dohalská L, Hodek P, Stiborová M, Collect Czech Chem Commun 2000;65:122–132.
[17] Stiborová M, Bořek-Dohalská L, Hodek P, Mráz J, Frei E, Arch Biochem Biophys 2002;403:41–49.
[18] Lightning LK, Jones JP, Friedberg T, Pritchard MP, Shou M, Rushmore TH, Trager WF, Biochemistry 2000;39:4276–4287.
[19] Nelson DR, Strobel HW, J Biol Chem 1988;263:6038–6050.
[20] Lewis DF, Xenobiotica 1998;28:617–661.
[21] Ekins S, De Groot MJ, Jones JP, Drug Metab Dispos 2001;29:936–944.
[22] Williams PA, Cosme J, Sridhar V, Johnson EF, McRee DE, Mol Cell 2000;5:121–131.
[23] Williams PA, Cosme J, Ward A, Angove HC, Vinkovic DM, Jhoti H, Nature 2003;424:464–468.
[24] Scott EE, He YQ, Wester MR, White MA, Chin CC, Halpert JR, Johnson EF, Stout CD, Proc Natl Acad Sci USA 2003;100:13196–13201.
[25] Antonovič L, Hodek P, Smrček S, Novák P, Šulc M, Strobel HW, Arch Biochem Biophys 1999;370:208–215.
[26] Bridges A, Gruenke L, Chang YT, Vasker IA, Loew G, Waskell L, J Biol Chem 1998;273:17036–17049.
[27] Domanski TL, Halpert JR, Curr Drug Metab 2001;2:117–137.
[28] Spatzenegger M, Wang Q, He YQ, Wester MR, Johnson EF, Halpert JR, Mol Pharmacol 2001;59:475–485.
[29] Chang Y-T, Stiffelman OB, Vakser IA, Loew GH, Bridges A, Waskell L, Protein Eng 1997;10:119–129.
[30] Dai R, Pincus MR, Friedman FK, J Protein Chem 1998;17:121–129.
[31] Wang Q, Halpert JR, Drug Metab Dispos 2002;30:86–95.
[32] Hodek P, Sopko B, Antonovič L, Šulc M, Novák P, Strobel HW, Gen Physiol Biophys 2004;, in press.
[33] Olah GA, Wu A, Farooq O, Prakash GKS, J Org Chem 1990;55:1792–1796.
[34] Guengerich FP, J Biol Chem 1977;252:3970–3979.
[35] Omura T, Sato R, J Biol Chem 1964;239:2370–2378.
[36] Anzenbacher P, Šípal Z, Hodek P, Biomed Biochim Acta 1984;43:1343–1349.
[37] Hodgson AV, Strobel HW, Arch Biochem Biophys 1996;325:99–106.
[38] Williams CH, Kamin H, J Biol Chem 1962;237:587–595.
[39] Vermilion JL, Coon MJ, J Biol Chem 1978;253:8812–8819.
[40] Wiechelman KJ, Braun RD, Fitzpatrik JD, Anal Biochem 1988;175:231–237.
[41] Lubet RA, Meyer RT, Cameron JW, Nims RW, Burke MD, Wolff T, Guengerich FP, Arch Biochem Biophys 1985;238:43–48.
[42] Burke MD, Thompson S, Elcombe OR, Halpert J, Haaparanta T, Mayer RT, Biochem Pharmacol 1985;34:3337–3345.
[43] Bořek-Dohalská L, Hodek P, Šulc M, Stiborová M, Chem Biol Interact 2001;138:85–106.
[44] Jefcoate CR In: Flescher S, Packer L, editors. Methods in Enzymology., 52 New York: Academic Press; 1978. p 258–279.
[45] Hodek P, Strobel HW, Bioorg Chem 1994;22:253–267.
[46] Podust LM, Kim Y, Arase M, Neely BA, Beck BJ, Bach H, Sherman DH, Lamb DC, Kelly SL, Waterman MR, J Biol Chem 2003;278:12214–12221.
[47] Sevrioukova IF, Li H, Zhang H, Peterson JA, Poulos TL, Proc Natl Acad Sci USA 1999;96:1863–1868.
[48] Morris GM, Goodsell DS, Halliday RS, Huey R, Hart WE, Belew RK, Olson AJ, J Comp Chem 1998;19:1639–1662.
[49] Lewis DFV, Eddershaw PJ, Dickins M, Tarbit MH, Goldfarb PS, Chem Biol Interact 1998;115:175–199.
[50] Chang Y-T, Stiffelman OB, Loew GH, Biochimie 1996;78:771–779.
[51] White RE, McCarthy MB, Egeberg KD, Sligar SG, Arch Biochem Biophys 1984;228:493–502.
[52] Johnston SL, Virus Res 2002;82:147–152.
[53] Blanchet PJ, Metman LV, Chase TN, Adv Neurol 2003;91:251–257.
[54] Yano JK, Wester MR, Schoch GA, Griffin KJ, Stout CD, Johnson EF, J Biol Chem 2004;279:38091–38094.
[55] Wester MR, Yano JK, Schoch GA, Yang C, Griffin KJ, Stout CD, Johnson EF, J Biol Chem 2004;279:35630–35637.
[56] Scott EE, White MA, He YA, Johnson EF, Stout CD, Halpert JR, J Biol Chem 2004;279:27294–27301.